Electromagnetic Penetration of Structures with Applications in Vulnerability Assessment

David P. Mignardot[(1)](dmignard@vols.utk.edu), DaHan Liao[(2)], Larry C. Markel[(2)], Yilu Liu[(1,2)]
(1) The University of Tennessee, Knoxville, TN 37996, USA, https://www.utk.edu
(2) Oak Ridge National Laboratory, Oak Ridge, TN 37831, USA, https://www.ornl.gov

***Abstract*—Threat of weaponized electromagnetic pulse is of increasing concern especially regarding the operation of the electrical power system. In this study, computational electromagnetic simulations are conducted to develop an understanding of the interaction between a structure and plane wave electromagnetic radiation. Field results are numerically calculated using the method of moments and are formulated into a transfer function to determine the attenuation provided by the structure. Variables are altered and compared to determine criticality. The results obtained from this study serve as a collection of general observations which can be extended to more complicated simulations.**

I. Introduction

During the height of the Cold War, scientific experiments such as Starfish Prime were conducted to test high altitude nuclear bursts. Results from such tests revealed generation of high-altitude electromagnetic pulse (HEMP) of magnitudes higher than expected from nuclear bursts in the stratosphere and above. HEMP from tests like Starfish Prime affected engineered systems on the ground [1]. Due to recent escalated threats, further understanding of the potential effects from HEMP is of concern. Researchers have conducted studies on the hazards of HEMP and the associated vulnerabilities of the electric power grid [2], [3]. The studies concentrated on the bulk transmission system. Less knowledge exists regarding the vulnerability of power generation facilities.

This study aims to develop a foundational understanding of the electromagnetic penetration of structures. This study also identifies dominant variables which contribute to a 'worst case' scenario. Future researchers can utilize this foundational knowledge and expand to more complex cases. The scope of this study is to collect general observations from simplified models that can be applied to more complex facilities.

II. Parameters of Interest

A. Angle of Incidence

Problems involving HEMP possess many challenges including the uncertainty of multiple variables. For example, the location and orientation of a nuclear detonation and the propagating electromagnetic pulse (EMP) relative to a facility is likely to be unknown. The orientation, with respect to a reference axis, of the incoming electromagnetic (EM) wave is known as the angle of incidence (AoI). The excitation source's angle of incidence dictates the interaction with the structure. In cases of variable uncertainty, the 'worst case' scenario is determined. In this paper, the AoI is measured with respect to the vertical axis as in Fig. 1; a straight downward propagation is represented with a zero-degree AoI.

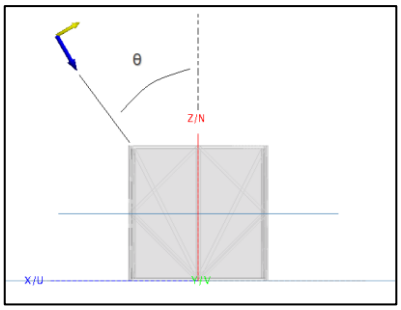

Figure 1. Angle of incidence θ measured with respect to vertical axis.

To analyze the effect of AoI, and alternate variables, electromagnetic simulations were run using *Altair FEKO* software. Method of Moments (MoM) is the default solver for this software and was used for all simulations. Garg provides a description of the MoM procedure in [4]. The simulations modeled the excitation source as plane wave propagation and provided nearfield results. For this case, the software simulated a hollow 10 m by 3 m by 4 m rectangular structure with 10cm thick walls (including floor and ceiling). A frequency independent wall material (ε_r = 4.5, σ = 0.02 S/m) was employed to emulate concrete. The vast majority of energy from a HEMP event is contained in frequencies below 100 MHz [2], [3]. Due to computational demands and knowledge of the HEMP spectral density, a frequency range from 100 kHz to 50 MHz was studied. The software automated meshing was used which defines the mesh based on 1/12 of the shortest wavelength [5]. An example of the mesh is pictured in Fig. 2.

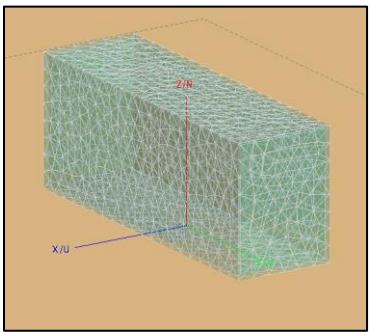

Figure 2. Example of the software's auto defined mesh.

A transfer function was developed by taking a ratio of the field data at the geometric center (single point) and the free space field value (1 V/m and 1/120π A/m for electric and magnetic field respectively). Decibel scaling was used for improved interpretation of results.

$$E_f = 20\log\left(\frac{E_p}{E}\right) \quad (1)$$

$$H_f = 20\log\left(\frac{H_p}{H}\right) \quad (2)$$

The transfer function results for a model with a perfect electric conducting (PEC) ground plane are plotted below in Fig. 3.

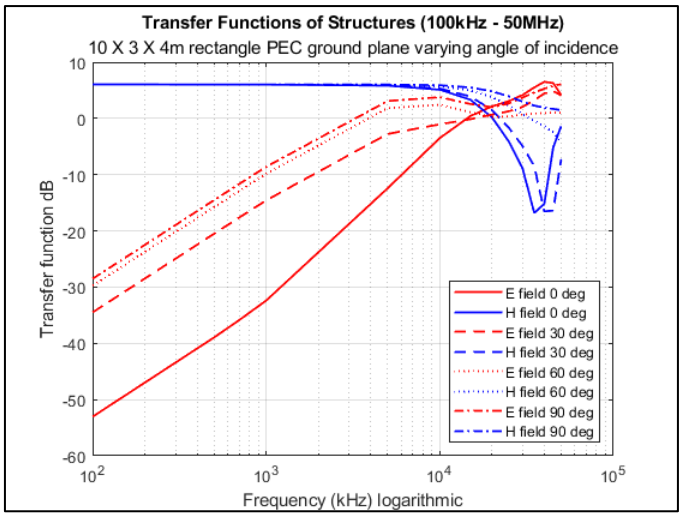

Figure 3. Comparison of transfer functions with varying angle of incidence.

A frequency independent dielectric ground plane was also modeled to emulate soil ($\varepsilon_r = 10$, $\sigma = 0$ .002 S/m). Results are plotted in Fig. 4.

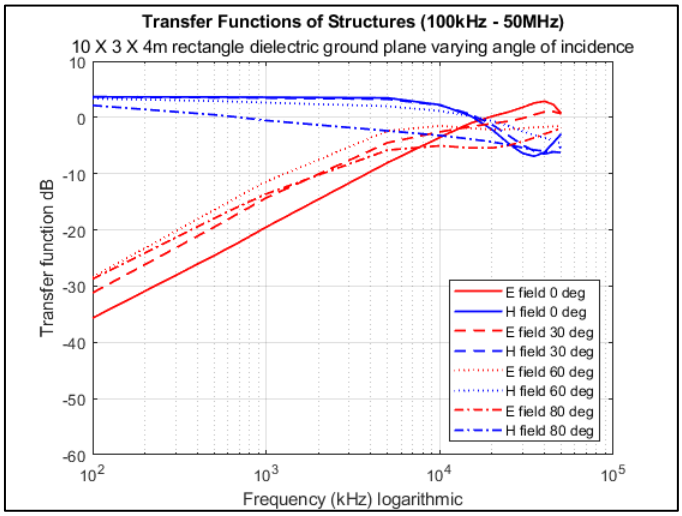

Figure 4. Comparison of transfer functions with varying angle of incidence for a case with a dielectric ground plane.

Recall the transfer function represents a ratio therefore, a large negative number implies the inside field data is very small compared to the free space value. Values below zero signify attenuation. The apparent amplification of the magnetic field is not an amplification but rather a result due to the definition of the transfer function. The ratio is taken with respect to the free space field value, and the calculated data includes the free space plus the reflected field values. Due to the magnetic boundary condition, the calculated field value is double the free space value hence the ~6 dB gain. In the low frequency region, the results indicate little variation with a change in AoI. The outlying curves are associated with angles at the extreme of the range (either 0° or 90°). It is worthy to note during an EMP event the AoI will be unknown and is more likely to be a moderate angle closer to the middle of the range. In the resonance region, larger angles appear to result in a less dramatic oscillatory effect. When observing the data in an average sense both ground plane scenarios generate similar results.

B. Polarization Angle

The polarization angle characterizes the time varying orientation of the electric field component of the incident electromagnetic wave. A wave can be vertically or horizontally polarized which corresponds to the electric field being parallel or perpendicular to the plane of incidence respectively. When considering a plane wave, both fields will propagate along the same axis. The angle of polarization is an important parameter to study because the polarization may affect the propagation characteristics of the wave and thus the penetration into the structure.

During an EMP event, the polarization will be unknown. Therefore, it is reasonable to determine a 'worst case' scenario for simulation efforts. Studying electromagnetic boundary conditions reveals the behavior of a plane wave when interacting with a conducting surface such as the earth. At the surface of a PEC (assuming an infinite half-space model), electric (E) fields consist of only normal components whereas magnetic (H) fields only consist of tangential components [6].

$$E_{tan} = 0 \quad (3)$$

$$H_n = 0 \quad (4)$$

Although the above conditions are observed at the surface, the observations can be extended to locations near the surface for approximate results. When analyzing the low frequency region, wavelengths can be orders of magnitude larger than the structure dimensions. Therefore, in lower frequency conditions, points around the structure are very close to the ground plane surface compared to the wavelength. To further validate the boundary conditions simulations were carried out to analyze field strength at various polarizations. When the incoming wave is horizontally polarized, the E field contains only tangential components regardless of AoI. The same is true for the H field if the incoming wave is vertically polarized. To illustrate the effect of polarization, field results were numerically calculated and averaged inside the walls of a 3 m cubical concrete structure. Figures 5 and 6 plot the field results

as a function of angle of incidence while comparing vertical (solid line) and horizontal polarization (dashed line).

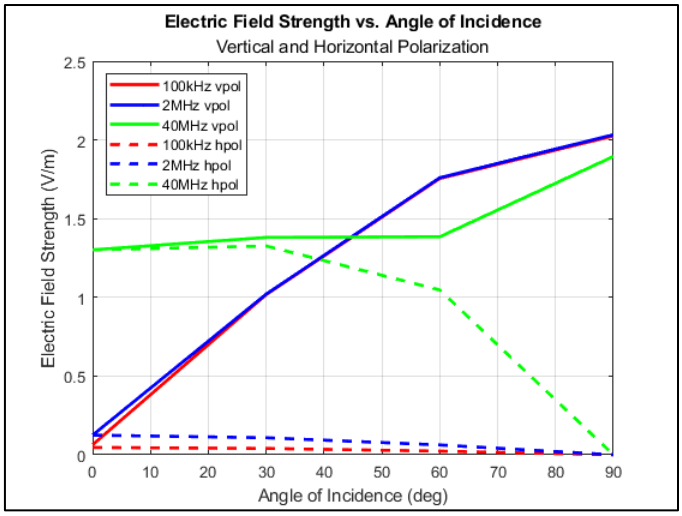

Figure 5. Electric field inside the structure.

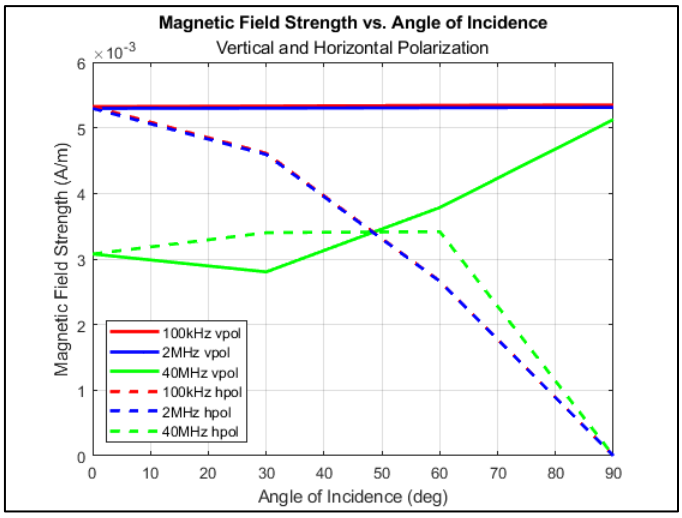

Figure 6. Magnetic field inside the structure.

It is evident the vertically polarized case enables the most intense excitation as the H field intensity is a constant value about twice the incident value. With the horizontally polarized case, the E field excitation is roughly zero regardless of AoI for lower frequencies. It is worthy to note the apparently increasing E field strength in the vertically polarized case is actually an oscillatory behavior as a function of distance. The field strength experiences maxima every quarter of a wavelength above the surface as demonstrated in Fig. 7 below.

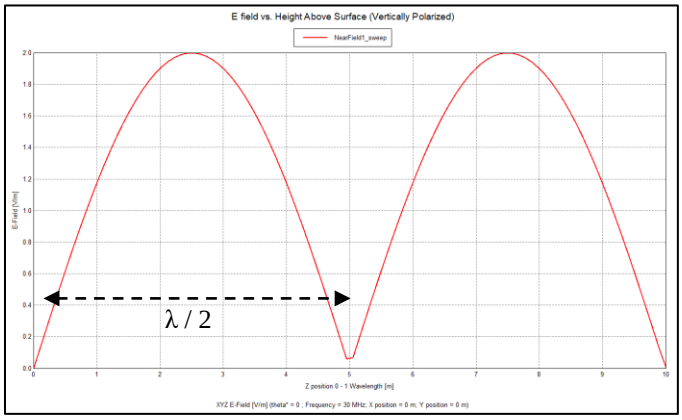

Figure 7. Electric field vs. height above surface (vertically polarized).

Employing a moderate polarization angle between vertical and horizontal does not constitute a 'worst case' scenario because for most incidence angles, tangential and normal field components will always exist. Although the polarization angle of an incoming EMP is likely to be unknown, assuming vertical polarization is a logical assumption. Vertical polarization enables a 'worst case' scenario as field strengths are observed to be most intense for a given frequency and angle of incidence. In the low frequency region, locations within the structure are close to the ground plane surface (with respect to wavelength) and therefore, observations can be expected to replicate that of boundary conditions.

C. Frequency Dependence of Wall Material

The previously discussed simulations employed a frequency independent wall material with a fixed permittivity and conductivity to emulate concrete. Further studies were conducted to determine if the frequency independent electrical parameter approximation was reasonable. A 10 m by 3 m by 4 m rectangular structure with an all-around wall thickness of 20 cm was modeled. Two comparisons were studied; the first comparing a frequency dependent software defined dielectric media, *construction concrete block*, and the previously used frequency independent material. The software defined media specifies data for a list of frequencies. Data from frequencies not specified is linearly interpolated [5]. A plane wave source propagated directly down onto the structure (0° angle of incidence) and a frequency range of 100 kHz to 50 MHz was analyzed. Data for the transfer function was averaged from nine points evenly spaced inside the walls of the structure. Results demonstrated a similar excitation behavior regardless of wall material especially for the magnetic field. The electric field experienced slightly less attenuation throughout the frequency spectrum under the frequency dependent media. Fig. 8 illustrates the transfer function results for this scenario.

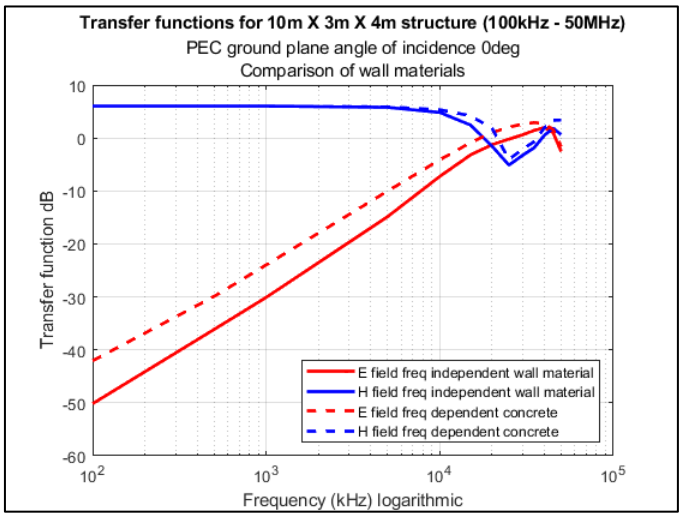

Figure 8. Comparison of transfer functions for different structure wall materials.

The second comparison studied the same frequency independent wall material compared to a frequency dependent media defined by the Messier Model. The Messier Model provides analytical expressions for conductivity and permittivity as a function of frequency [7], [8]. The expressions are defined in equations (5) and (6) below.

$$\sigma(f) = \sigma_{DC}\left(1 + \sqrt{\frac{4\pi f \varepsilon_\infty}{\sigma_{DC}}}\right) \quad (5)$$

$$\varepsilon_r(f) = \frac{\varepsilon_\infty}{\varepsilon_0}\left(1 + \sqrt{\frac{\sigma_{DC}}{\pi f \varepsilon_\infty}}\right) \quad (6)$$

σ_{DC} is the DC conductivity and was set to 6.5e-3 S/m. ε_∞ is the high frequency limit of the dielectric and is set to 8 times ε_0. In this simulation a 50° angle of incidence was utilized and data for the transfer function was averaged over a volume inside the structure including 96 points. Fig. 9 illustrates the data point locations.

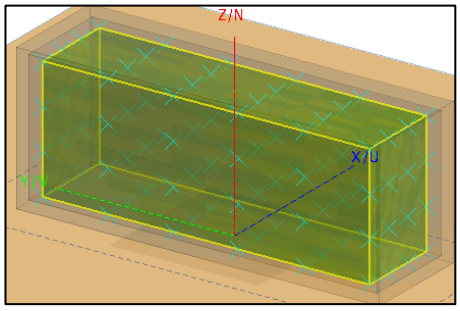

Figure 9. Points within structure at which field results were calculated.

The results from the second comparison agreed well with the first as can be seen in Fig. 10 below. Little influence from the frequency dependence of the wall material's electrical properties was observed. The Messier Model defined media behaved nearly identical to the software defined media demonstrating slightly less attenuation when compared to the frequency independent wall material.

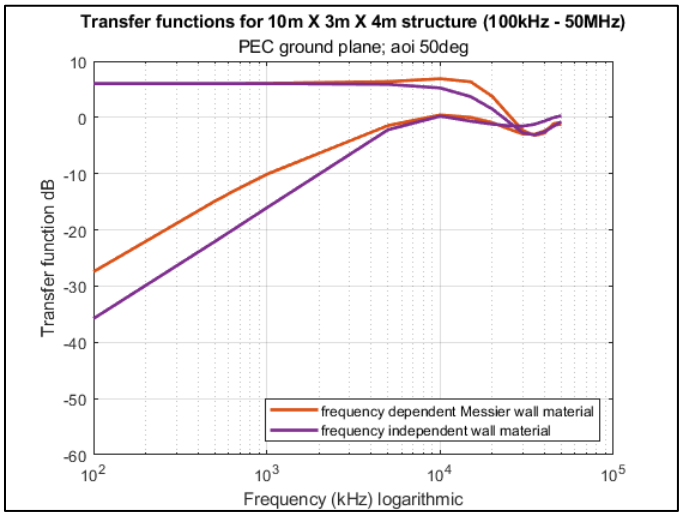

Figure 10. Comparison of transfer functions for different structure wall materials.

When assuming the Earth as a PEC, and performing simulations in the 100 kHz – 50 MHz range, frequency dependence of the wall material's electrical properties does not significantly alter transfer function results. It is a reasonable simplification to assume constant permittivity and conductivity for the structure's construction material. The software defined media and a material characterized by the Messier Model exhibit very similar results.

D. Effect of Dielectric Ground Plane

Scientists assume Earth to be a perfect electrical conductor for a wide variety of electromagnetic and geophysical studies such as in [9] and [10]. This assumption is valid because the earth acts as infinite source of charge. However, the earth is not a perfect conductor and maintains some electric field beneath the surface. Many variables influence the earth's electrical properties as Vance points out in [11]. Simulations were conducted to analyze the validity of a PEC ground plane by comparing transfer function results with two dielectric ground plane models. A frequency independent dielectric ground plane was modeled (ε_r = 10, σ = 0.002 S/m), as well as a frequency dependent dielectric ground plane defined by the Messier Model using a DC soil conductivity of 0.002 S/m. [7]. Geology consistent with the Eastern Tennessee region was taken to approximate these electrical properties. This geology consists of rocky hill terrain composed of primarily sedimentary rocks such as limestone and dolomite; and topsoil is considered a mixture of loam and sand. [11]–[16]. A 3 m cubical structure with an all-around wall thickness of 10 cm was modeled. Data for the transfer function was averaged over 64 points in a volume centered inside the structure walls. A comparison of the transfer function results is pictured in the Fig. 11 below. A visual representation of electric field results is displayed in Fig. 12.

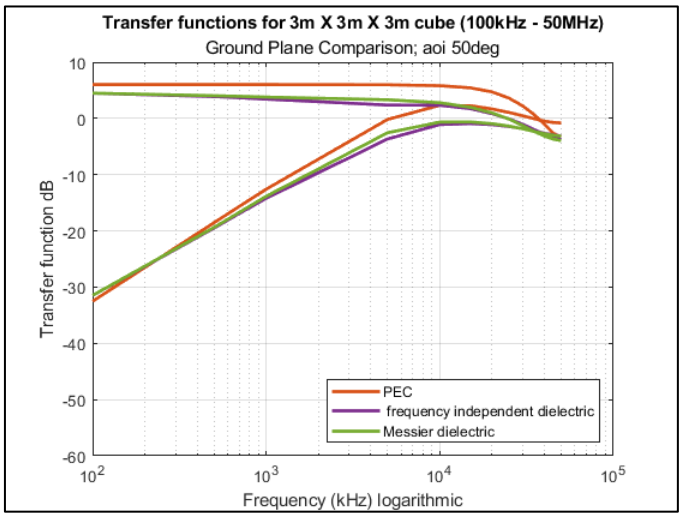

Figure 11. Comparison of transfer functions for different ground planes.

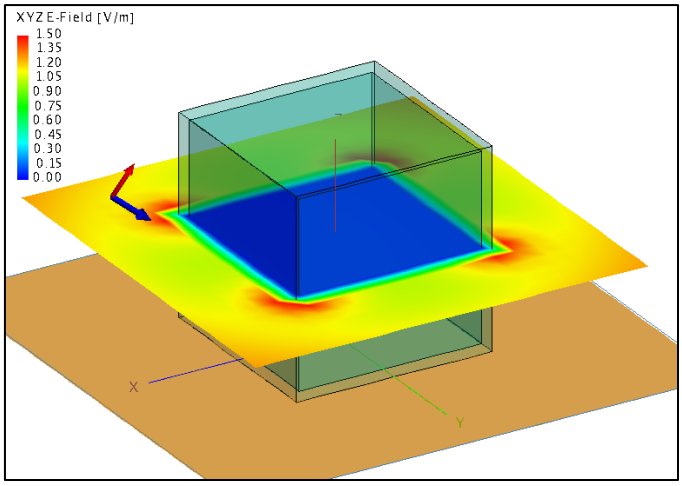

Figure 12. Electric field results inside and around structure for PEC ground plane (100 kHz).

Simulation errors were observed when employing a dielectric ground plane. 'Hot spots' of high intensity field appeared near the walls inside of the structure at frequencies around and below 1 MHz. These results are likely erroneous and express a limitation of the MoM solver. One potential contributor to the inaccuracies is the solvers inability to converge accurate solutions of the Sommerfeld integrals at lower frequencies. When data was taken away from the walls, results demonstrated precision with the alternate simulations conducted in this study. Fig. 13 pictures the inaccurate 'hot spots'.

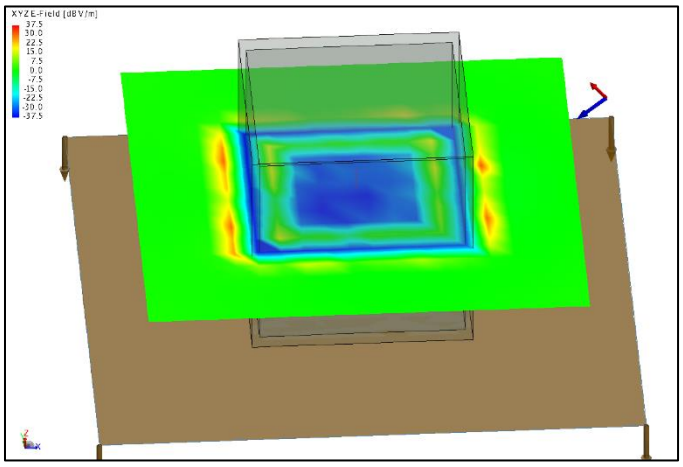

Figure 13. Electric field results inside and around structure for dielectric ground plane (100 kHz).

The assumption to utilize a PEC ground plane does not drastically affect results when studying this particular frequency range. In fact, the PEC model provided the lowest attenuation. As the frequency approaches the resonance region, results tend to diverge more. The dielectric ground plane models behaved very similarly throughout the frequency range and thus the frequency dependence of the ground plane is not a significant parameter in this study. It is worthy to note the dielectric ground plane models take more computation time due to the solving of Sommerfeld integrals in the MoM.

III. Conclusions

This work has studied several variables and their influence on electromagnetic penetration of structures associated with high-altitude electromagnetic pulse. Variation with the angle of incidence of the incoming radiation has little influence on the fields observed inside the structure especially when considering an averaged angle in the middle of the range. Strongest coupling effects are expected when the incoming radiation is vertically polarized because of the total magnetic field excitation. It was also observed for lower frequencies, excitation behavior replicated that of surface boundary condition behavior. When considering a structure's wall material, frequency dependence of the electrical properties does not constitute significant differences in transfer function results. Using a frequency independent model or a software defined media is reasonable. The same statement can be made regarding dielectric ground planes. No significant difference was observed when comparing a perfect electric conductor and dielectric ground plane, especially in the low frequency region. It is worthy to note the H field remains roughly constant throughout the low frequency region. However, the E field attenuation decreases quadratically as a function of frequency. This general behavior serves as a baseline for future studies. Overall, these results provide reasonable assumptions which can be applied as simplifications when studying more complex cases.

References

[1] *Report of the Commission to Assess the Threat to the United States from Electromagnetic Pulse*, Vol. I. Executive Report, April 2004.

[2] *High-Altitude Electromagnetic Pulse and the Bulk Power System: Potential Impacts and Mitigation Strategies.* EPRI, Palo Alto, CA: 2019. 3002014969.

[3] E. Savage, J. Gilbert, and W. Radasky, *The Early-Time High-Altitude Electromagnetic Pulse and its Impact on the U.S. Power Grid.* Metatech Corporation, Goleta, CA: 2010.

[4] R. Garg, "Method of moments," in *Analytical and Computational Methods in Electromagnetics*, Massachusetts: Artech House, 2008.

[5] *User Manual for FEKO 14.0.* Altair, HyperWorks, Dec. 2015.

[6] F. T. Ulaby, E. Michielssen, and U. Ravaioli, "Maxwell's equations for time-varying fields," in *Fundamentals of Applied Electromagnetics*, 6th ed., Boston: Prentice Hall, 2010, pp. 301.

[7] D. Cavka, N. Mora, F. Rachidi, and D. Poljak, "On the application of frequency dependent soil models to the transient analysis of grounding electrodes," in *Proc. Int. Symp. Electromagnetic Compatability*, Brugge, Belgium, Sep. 2013.

[8] M. Messier, "Another soil conductivity model," Internal Report, Jaycor, Santa Barbara, CA, 1985.

[9] R. G. Olsen and P. S. K. Wong, "Characteristics of low frequency electric and magnetic fields in the vicinity of electric power lines," in *IEEE Transactions on Power Delivery*, Vol. 7, no. 4, pp. 2046-2055, Oct. 1992.

[10] A. K. Kamra and M. Ravichandran, "On the assumption of the Earth's surface as a perfect conductor in atmospheric electricity," in *Journal of Geophysical Research*, Vol. 98, no. D12, pp. 22875-22885, Dec. 1993.

[11] E. F. Vance, "Wave interaction with the soil," in *Coupling to Shielded Cables*, Wiley, 1978.

[12] G. V. Keller and F.C. Frischknecht, "Electrical methods in geophysical prospecting," New York: Pergamon Press, 1966.

[13] R. J. Lytle, "Measurement of earth medium electrical characteristics: techniques, results, and applications," in *IEEE Transactions on Geoscience Electronics*, vol. 12, no. 3, pp. 81-101, July 1974

[14] E. I. Parkhomenko, "Electrical properties of rocks," Plenum Publ. Corp, 1967.

[15] USGS, Tennessee Geologic Map Data, Retrieved November 8, 2022, from https://mrdata.usgs.gov/geology/state/state.php?state=TN

[16] U.S. Department of the Interior, National Parks Service, *Geology*, November 8, 2022, from https://nps.gov/grsm/learn/nature/geology